

AN EFFICIENT SYNTHETIC ROUTE, CHARACTERIZATION AND ANTIMICROBIAL EVALUATION OF Co(II), Ni(II), Cu(II) and Zn(II) SCHIFF BASE COMPLEXES

Salihu Sani^{1,3*}, Ibrahim Tajo Siraj², Mukhtar Atiku Kurawa² and Siti Nadiah Abdul Halim³

¹Department of Pure and Applied Chemistry, Usmanu Danfodiyo University, P.M.B. 2346,
Sokoto, Nigeria

²Department of Pure and Industrial Chemistry, Bayero University Kano, P.M.B 3011, Kano,
Nigeria

³Department of Chemistry, University of Malaya, 50603 Kuala Lumpur, Malaysia

(Received April 27, 2022; Revised July 3, 2022; Accepted July 3, 2022)

ABSTRACT. The synthesis of Schiff base compound derived from 2-hydroxy-3-methoxybenzaldehyde and *o*-phenylenediamine via solvent-assisted mechanochemical synthesis in the presence of a small amount of dimethylformamide as liquid-assisted solvent was reported. The Co(II), Ni(II), Cu(II) and Zn(II) Schiff base complexes were synthesized and characterized by powder x-ray diffraction, infra-red spectroscopy, differential scanning calorimetry, thermogrametric analysis, energy dispersive X-ray analysis and CHNS/O macro-analysis. According to infrared spectral analysis, a strong band in the spectra of Schiff base at 1617 cm⁻¹ was assigned to the azomethine $\nu(\text{C}=\text{N})$ stretching vibration. In the complexes, it shifted to lower frequency regions, indicating the formation of desired compounds. The DSC thermogram of Schiff base showed a single sharp peak at 158 °C, which is attributed to the melting or the phase transition. As revealed by TGA, the complexes were obtained as solid compounds containing some amounts of water molecules. The powder-XRD analysis showed that the patterns of the synthesized compounds were different from the starting materials, indicating that the starting constituents were changed into product. The antimicrobial activity results for selected bacteria and fungi revealed that complexes have higher activity than the Schiff base. Furthermore, the synthesized compounds were found to be more effective against fungal isolates than those of bacteria.

KEY WORDS: Schiff base, Solvent-assisted mechanochemistry, Azomethine, Complexes

INTRODUCTION

The conventional solvent-based syntheses involve the transformation of reactants into products in the presence of solvents (mostly organic solvents). The solvent(s) act as a medium through which the reactant molecules interact with each other and transform into product. However, the dependence on the use of solvents appears increasingly unsustainable since it is uneconomical (most of them are hazardous, energy-demanding, and environmentally problematic) [1, 2]. These problems have triggered the development of mechanochemical methods as a substitute to solvent-based methods. The mechanochemical method requires little or no addition of solvents and the transformation of solid precursors into products is made by the input of mechanical force, such as grinding, ball milling, surface rubbing, shearing, etc. [3]. Some reactions were found to progress more rapidly under solid state mechanochemical conditions as compared to solvent-based methods. For instance, if one of the reactant components is a hydrate, which produces water during the reaction, or if liquid by-products such as acetic acid or water are produced during the reaction, thus generated liquid may accelerate the reaction [4-7]. Inspired by this, a small amount of solvent is intentionally added to the reaction mixture during the mechanochemical process. Subsequent research studies have revealed that addition of a small quantity of appropriate solvent can intensely enable and accelerate mechanochemical reactions between solid reactants [8, 9].

*Corresponding author. E-mail: salihusani016@gmail.com

This work is licensed under the Creative Commons Attribution 4.0 International License

Schiff bases are formed by the condensation reaction of a primary amine with an aldehyde or ketone under certain conditions. Schiff base ligands and their transition metal complexes play an important role in the field of bioinorganic chemistry as antimicrobial agents. The salen-type ligands have various active donor sites in the aromatic ring which offer the architectural attractiveness to the metal centre to form coordination complexes [10-20]. The transition metal complexes derived from these types of ligands advanced due to their structural flexibility and chelating ability with a lot of interesting pharmacological activities, antibacterial, antifungal, antimalarial and antiviral activities [21-28]. The synthesized Schiff base and complexes were tested to evaluate their inhibitory activity towards the growth of pathogenic bacteria (*Staphylococcus aureus*, *Escherichia coli*) and fungal pathogens (*Aspergillus flavus*, *Aspergillus niger*).

To our knowledge, this article is the first report of solvent-assisted mechanochemical synthesis of Schiff base derived from 2-hydroxy-3-methoxybenzaldehyde and *o*-phenylenediamine and its Co(II), Ni(II), Cu(II) and Zn(II) complexes. The synthetic technique has been overlooked in the past, but it is becoming increasingly obvious that it is successful and even more advantageous in a growing number of synthetic reactions.

EXPERIMENTAL

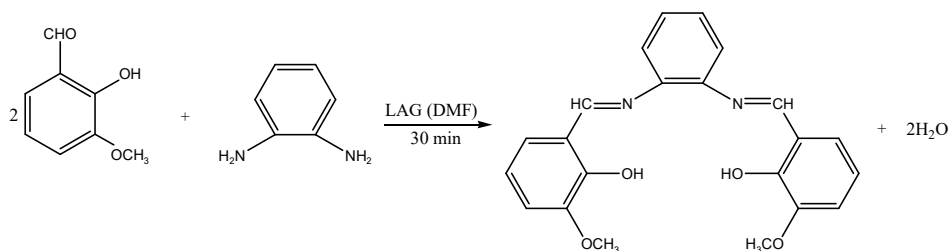
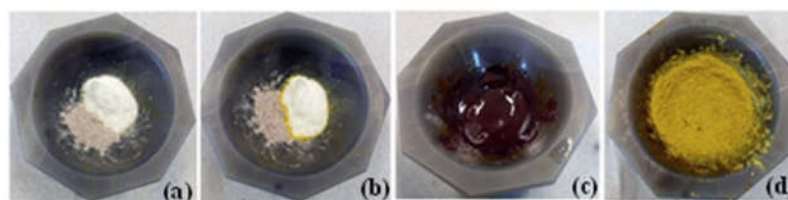
Reagents-grade chemicals and solvents used in this particular study were purchased from Sigma Aldrich UK in > 95% purity. Materials were actually used as received without further purification. FT-IR spectra of the samples were recorded using the Perkin-Elmer infrared Spectrum-400. Powdered X-ray diffraction patterns (PXRD) were recorded using PANalytical Empyrean X'Pert Pro x-ray diffractometer. The Diffractograms were carried out from 5 to 60° with a steep angle of 0.0167° per second. Energy dispersive X-ray (EDX) spectra were recorded using a Hitachi field emission scanning electron microscope (FESEM/EDX, SU8220). Differential scanning calorimetry (DSC) was carried out using the TA DCS Q20 V24.10 equipped with cooling accessories from -180 to 350 °C. The thermal stability of the complexes was studied using Perkin-Elmer Pyris diamond TG/DTA at a heating rate of 10° min⁻¹ under the flow of nitrogen gas (200 mL min⁻¹). Electronic absorption spectra were recorded using a Shimadzu UV-Vis 240 spectrophotometer. The bulk elemental composition of the samples was accessed using a Perkin-Elmer CHNS/O 2400 series II elemental analyzer. All the analyses were carried out at the Department of Chemistry, University of Malaya, Malaysia.

Synthesis of Schiff base

The Schiff base (H₂L¹) was synthesized by the reaction between 2-hydroxy-3-methoxybenzaldehyde and *o*-phenylenediamine (Scheme 1). In a typical synthesis, 1.52 g (10 mmol) of 2-hydroxy-3-methoxybenzaldehyde and 0.54 g (5 mmol) of *o*-phenylenediamine were weighed into an agate mortar. The sample was ground with a mortar and pestle, and a small quantity of dimethylformamide (DMF), methanol, or water (generally, one drop) was added to enable paste formation. An orange-coloured product was obtained after 30 min of continuous grinding. The final product was left to dry in the air (Plate 1) and then recrystallize. As a control, the procedure was repeated under the same conditions but without the addition of solvent.

Synthesis of complexes

About 0.38 g (1 mmol) of Schiff base (H₂L¹) and 1 mmol of metal acetate, (M(CH₃COO)₂·nH₂O, where M = Co, Ni, Cu or Zn and n is the number of hydrated water) were weighed into agate mortar and a drop of DMF was added. The composition was ground for 30 min to obtain coloured compounds. The compounds were air dried at room temperature and then recrystallize.

Scheme 1. Synthetic reaction of Schiff base (H₂L¹).Plate 1. Digital photograph of (a) reactants, (b,c) intermediate, and (d) Schiff base (H₂L¹), showing the steady changes in colour of the reactants and the formation of Schiff base.*Antimicrobial activity test*

The microbial isolates were collected from the Aminu Kano Teaching Hospital's Department of Chemical Pathology in Kano, Nigeria, and were identified using Gram staining and biochemical tests. The antimicrobial activities of Schiff base and metal complexes in dimethylsulfoxide (DMSO) were investigated *in vitro* using the agar well diffusion method according to the method described by Yusaha'u and Sadiu [29].

RESULTS AND DISCUSSION

The first attempt to synthesize the Schiff base by the neat grinding of the reactants in the absence of any solvent for 30 min resulted in the formation of a mixture comprising solid reactants only. Even after 80 min of neat grinding, no trace of a new compound was detected. It has been reported that the deliberate addition of a small quantity of liquid can enhance the scope and rate of mechanochemical synthesis significantly [30, 31]. In view of this, a drop of DMF was introduced to the reactants, followed by grinding for 30 min. As expected, the powder X-ray diffraction of Schiff base synthesized in the presence of DMF solvent differed significantly from that of the starting materials, a clear indication that the raw starting materials have been successfully converted into products. Clearly, a sharp and intense peaks observed at 13.032° and 8.712° in the powder X-ray diffraction spectra of 2-hydroxy-3-methoxybenzaldehyde and *o*-phenylenediamine, respectively, are absent in the spectrum of the product. Instead, at 8.339°, 18.471° and 20.273°, new sharp and intense peaks were observed which also implies the formation of the Schiff base (Figure 1). The sharp reflections in the PXRD patterns of Schiff base suggests crystallinity of the products [30]. To further explore the most appropriate solvent for the formation of Schiff base with both high phase purity and percentage yield, another set of experiments were carried out using two different solvents namely; methanol (CH₃OH) and distilled water (H₂O). It is evident from the PXRD results that all the solvents result in the formation of the target Schiff base (the

measured PXRD patterns are identical, demonstrating that all the products were produced as pure single phases). However, the degree of crystallinity and phase purity of the as-synthesized Schiff base differ. Among all the solvents, DMF solvent results in the formation of a Schiff base with higher degree of crystallinity (more sharp peaks with high intensity) as compared to other solvents as evident from the PXRD spectra. Thus, in the present study, it is reasonable to suggest that DMF is the most appropriate solvent to synthesize the Schiff base with high crystallinity.

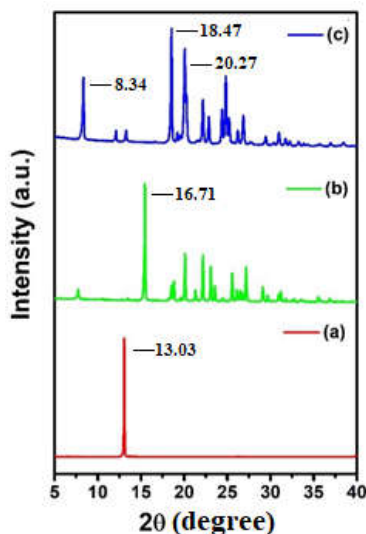


Figure 1. PXRD patterns of (a) 2-hydroxy-3-methoxybenzaldehyde, (b) *o*-phenylenediamine, and (c) Schiff base, indicating that the PXRD patterns of Schiff base is different from that of the reactants.

The complexes' diffractograms also show different reflection peaks in relation to the reactants. The similarity of the powder X-ray diffraction patterns of the synthesized complexes indicates their isostructural nature (Figure 2).

The liquid-assisted mechanochemical method adopted produced Schiff base and its metal complexes with a percentage yield in the range of 78.7–90.7% within a shorter reaction time of 30 min (Table 1). The Schiff base ligand and complexes prepared were coloured. Most complexes' colours are caused by electronic d-d transitions between energy levels [32]. Furthermore, all the metal complexes have a higher decomposition temperature (195–230 °C) than that of the Schiff base's melting point (158 °C), this implies that metal complexes are much more stable than the Schiff base. Complexation was found to be responsible for metal complexes' higher stability [32].

The FT-IR spectra recorded confirms the formation of Schiff base. Figure 3 shows that bands corresponding to the amino group (3363, 3184 cm^{-1}) and carbonyl group (1661 cm^{-1}) are absent in the IR spectrum of the Schiff base. Instead, a new band at 1617 cm^{-1} was observed, which corresponds to -C=N- of azomethine. The band observed at 1117 cm^{-1} in the IR spectrum of the Schiff base was assigned to C-O-C symmetric stretching in the methoxy group (R-O-CH_3). The strong band observed at 3371 cm^{-1} was assigned to O-H stretching vibration, whereas the band seen at 1203 cm^{-1} was attributed to phenolic C-O stretching [33].

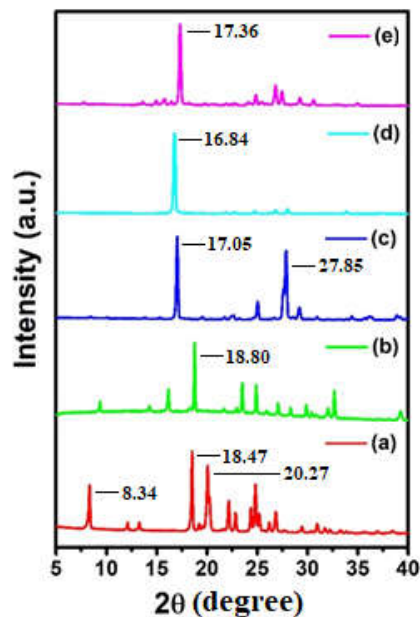


Figure 2. PXRD patterns of (a) Schiff base (H_2L), (b) $[Co(L)]$, (c) $[Cu(L)]$, (d) $[Ni(L)]$, and (e) $[Zn(L)]$ complex.

The prepared Schiff base's IR spectrum was compared to that of the complexes (Figure 4). For instance, a band at 1617 cm^{-1} in the Schiff base spectrum corresponding to the stretching vibration of azomethine ($-C=N-$) shifted to lower wave number values in the spectra of all the synthesized complexes ($1583\text{--}1593\text{ cm}^{-1}$). This signifies that azomethine nitrogen has been coordinated with the metal center [34]. In addition, the phenolic O–H band observed in the spectrum of Schiff base was absent in the spectra of complexes, instead, M–O bands were observed. Similarly, the band due to phenolic C–O stretching shifted in the spectra of complexes, indicating deprotonation and coordination of hydroxyl oxygen to the metal ion [35]. Further, the appearance of new bands in complexes' spectra in the range of $628\text{--}689$ and $450\text{--}533\text{ cm}^{-1}$ corresponds to M–N and M–O vibrations, respectively [36]. This also suggests that N and O atoms are involved in the complexation process [37].

Energy dispersive X-ray (EDX) analysis was used to study the surface elemental composition of the Schiff base and complexes. Only peaks corresponding to carbon, nitrogen, and oxygen were observed in the EDX spectrum of the Schiff base (Figure 5). Carbon has the largest atomic percent (72.95%), followed by oxygen (14.90%) and nitrogen (12.15%). The highest atomic percentage of carbon was due to the high content of atomic carbon in the synthesized Schiff base, which was further confirmed by the CHN analysis data. The atomic percentages of all the three component elements were compared at different points and the results were found to be consistent, showing that all of the constituent elements in the sample compound were distributed uniformly.

In addition to the peaks, which correspond to carbon, nitrogen and oxygen observed in the EDX spectrum of the Schiff base, peak corresponding to Co, Ni, Cu and Zn are also observed in the EDX spectrum of $[Co(L)]\cdot 3H_2O$, $[Ni(L)]\cdot 4H_2O$, $[Cu(L)]\cdot 3H_2O$ and $[Zn(L)]\cdot 2H_2O$ complexes respectively. Further, the relative percentage of the metal in the as-synthesized metal complexes follows the order; $[Zn(L)]\cdot 2H_2O$ (2.47%), $>$ $[Cu(L)]\cdot 3H_2O$ (2.02%), $>$ $[Ni(L)]\cdot 4H_2O$ (1.92%), $>$ $[Co(L)]\cdot 3H_2O$ (0.92%).

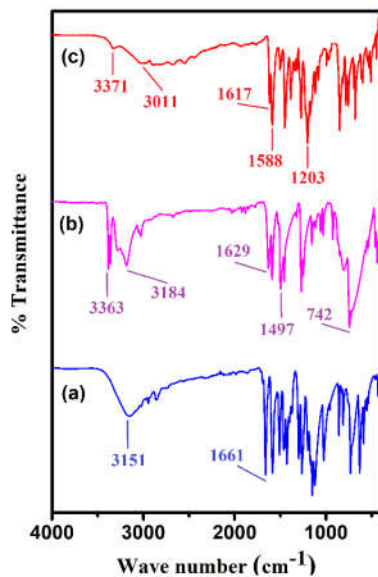


Figure 3. FT-IR spectra of (a) 2-hydroxy-3-methoxybenzaldehyde, (b) *o*-phenylenediamine, and (c) Schiff base (H_2L^1) indicating the formation of Schiff base.

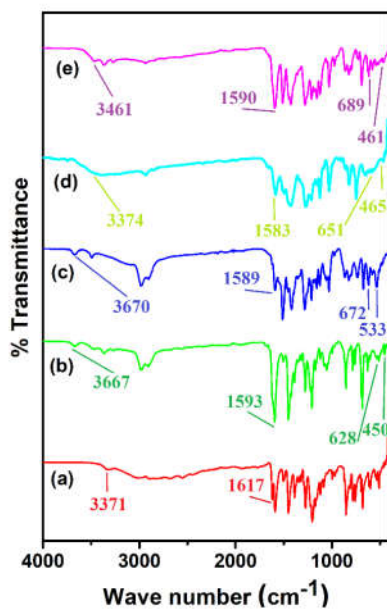


Figure 4. FT-IR spectra of (a) (H_2L^1), (b) $[Co(L^1)]$, (c) $[Cu(L^1)]$, (d) $[Ni(L^1)]$, and (e) $[Zn(L^1)]$ complexes indicating the formation of synthesized complexes.

The EDX result was compared to the CHN analysis result in terms of relative percentage. As expected, the relative percentages of nitrogen, oxygen, and carbon derived from EDX and CHN analysis are similar [38].

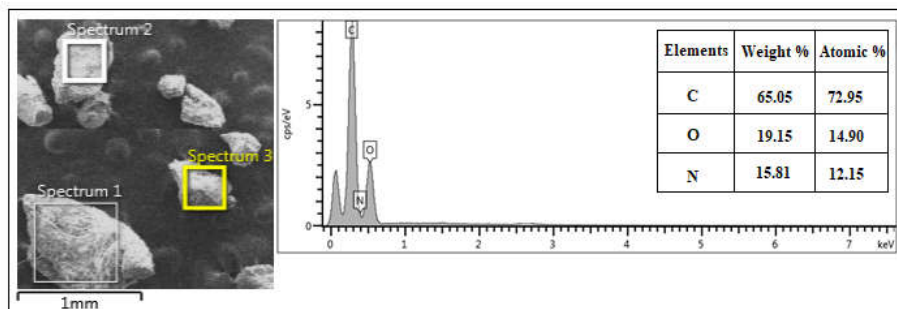


Figure 5. EDX spectrum of Schiff base with SEM image.

The experimental results for the thermal analysis of the complexes are summarized in Table 1. The product was obtained as solid compounds containing variable amounts of residual water molecules as shown by thermogravimetric analysis result. The results of the complexes' thermogravimetric analysis (TGA) and differential thermal analysis (DTA) are shown in Figure 6. The dotted line represents the differential thermal analysis (DTA), which validates the results of the TGA analysis (curve line). The advantage of using a synchronizing apparatus is that the sample and experimental conditions are the same, allowing for easy comparison of data.

Figure 6a depicts the thermal decomposition of $[\text{Co}(\text{L}^1)] \cdot 3\text{H}_2\text{O}$ complex. The initial weight loss of 8.43% observed at 107 °C in the thermogram of the complex corresponds to the removal of three molecules of water, and this is consistent to the calculated result of 9.30%. The second weight loss, followed by an exothermic peak, observed in the temperature range between 175 and 220 °C with mass loss of 9.66%, corresponds to the limitation of O_2CH_3 component [39]. The complex is found to undergo gradual decomposition at around 250 °C (observed weight loss of 9.5%).

Within the temperature range of 45–400 °C, the thermogram of the $[\text{Ni}(\text{L}^1)] \cdot 4\text{H}_2\text{O}$ complex reveals three decomposition steps (Figure 6b). At 105 °C, the percentage weight loss (11.82%) corresponds to four molecules of water, based on the calculated result of 10.20%. The first decomposition occurs at 196 °C, with an estimated weight loss of 6.88%, corresponding to the loss of (OCH_3) , while the second decomposition occurs at 280 °C, with a mass loss of 13.02%, matching the theoretical weight loss of 11.00%.

The $[\text{Cu}(\text{L}^1)] \cdot 3\text{H}_2\text{O}$ complex is thermally decomposed in three steps. The practical weight loss of 12.87% corresponds to the loss of three residual water molecules at the 105 °C. The complex underwent further decomposition and gave another break at 230 °C with weight loss of 10.63% which corresponds to the decomposition of complex to expel (O_2CH_3) species. The degraded complex further went to decompose at 370 °C, with practical weight loss of 7.50% (Figure 6c). Study of the thermal decomposition process of the $[\text{Zn}(\text{L}^1)] \cdot 2\text{H}_2\text{O}$ complex shows the first practical weight loss of 6.77% at 105 °C, which corresponds to the loss of two residual water molecules. The complex decomposed at 195 °C. (Figure 6d). A similar justification was made by Khalil *et al.* [40].

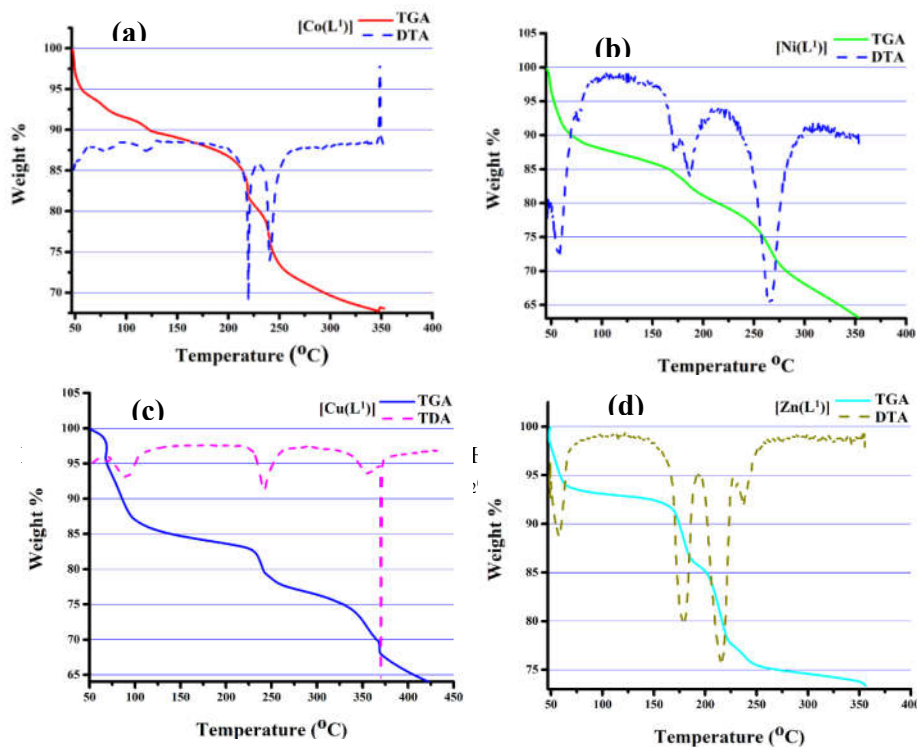


Figure 6. TGA/DTA Analysis of (a) $[\text{Co}(\text{L}^1)] \cdot 3\text{H}_2\text{O}$, (b) $[\text{Ni}(\text{L}^1)] \cdot 4\text{H}_2\text{O}$, (c) $[\text{Cu}(\text{L}^1)] \cdot 3\text{H}_2\text{O}$, (d) $[\text{Zn}(\text{L}^1)] \cdot 2\text{H}_2\text{O}$ complex.

At room temperature, the molar conductivity values of metal complexes in 10^{-3} M solution in ethanol were measured. The molar conductance (Λ_m) values of the metal complexes are shown in Table 1. From the results obtained, complexes have molar conductance values of 4.43–5.33 $\Omega^{-1}\text{cm}^2\text{mol}^{-1}$. The lower conductivity values indicates that it is non-electrolytic, since a 1:1 electrolyte is expected to have a value in the range of 75–90 $\Omega^{-1}\text{cm}^2\text{mol}^{-1}$ [41]. The chelates show no considerable conductance, and this supports their neutral nature.

As presented in Table 1, magnetic susceptibility measurements at room temperature reveal that Co(II), Ni(II), and Cu(II) complexes are paramagnetic in nature, with magnetic moments ranging from 1.733 to 2.328 BM. Kalia *et al.* obtained similar magnetic moment (2.12–2.31 BM) for Co(II) complexes of dithiocarbamate derived from isoniazid [42]. Based on Kalia *et al.* results for most square planar geometry surrounding Co(II) d^7 complexes, these values fall within the range of one unpaired electron. Literature study also reveals that the Cu(II), Ni(II) and Co(II), complexes showing the values of magnetic moment in the above range proposed the square planar stereochemistry around the metal(II) complexes [43, 44]. Hence the square planar geometry for Cu(II), Ni(II) and Co(II) complexes were proposed. The diamagnetic system revealed by the magnetic moment value of the Zn(II) complex corresponds to 0 unpaired electrons of d^{10} species. As a result, the Schiff base coordinates to the Zn(II) ion as a square-planar four-dentate chelating agent.

The UV-Visible spectra of the synthesized Schiff base ligand and complexes were recorded at room temperature in methanol (10^{-4} M) in the range of 185 to 600 nm. The azomethine ($\text{C}=\text{N}$),

a chromophore, is expected to absorb at certain region in the UV-Vis spectroscopy ($n \rightarrow \pi^*$ transition). The $n \rightarrow \pi^*$ transition occurs because, non-bonding electron pairs on nitrogen (azomethine) undergo a hypochromic shift when coordinated to a metal ion [45]. The absorption of the azomethine functional group of a Schiff base was found to be at a lower energy (higher wave length) compared to that of metal complexes. The absorption spectrum of Schiff base consists of an intense band at 283 nm due to $\pi \rightarrow \pi^*$ transition of the benzene ring (Table 1). An additional intense band in the lower energy region of the spectrum of the Schiff base (364 nm) was related to the $n \rightarrow \pi^*$ transition of azomethine. A Similar transition ($n \rightarrow \pi^*$) was also observed in the spectra of complexes, however, it was moved to lower frequencies (355–360 nm), indicating Schiff base coordination with metallic ions. The obtained values for $\pi \rightarrow \pi^*$ and $n \rightarrow \pi^*$ transitions were comparable to the values stated by Joseyphus *et al.* [34]. The d-d transition in these types of complexes may appear above 500 nm but was not observed due to the low intensity of the d-d transition as reported by Khalil *et al.* [40].

Table 1. Properties, molar conductance, magnetic moment, electronic transition and CHN analysis of Schiff base complexes.

Compound	Colour	Melting point/ decomp. temp.(°C)	Yield (%)	Molar conductance ($\Omega^{-1}\text{cm}^2\text{mol}^{-1}$)	μ_{eff} (BM)	Electronic transition		Found (calculated) %		
						$\pi \rightarrow \pi^*$ (nm)	$n \rightarrow \pi^*$ (nm)	C	H	N
H ₂ (L ¹)	Orange	158	90.7	-	-	283	364	69.55 (70.20)	5.45 (5.36)	7.79 (7.44)
[Co(L ¹)]·3H ₂ O	Brown	220	87.4	4.60	1.733	265	355	60.52 (60.98)	4.36 (4.19)	6.58 (6.46)
[Ni(L ¹)]·4H ₂ O	Brown	196	89.9	5.33	2.328	263	357	60.72 (60.43)	4.35 (4.14)	6.69 (6.40)
[Cu(L ¹)]·3H ₂ O	Purple	230	78.7	4.56	2.199	260	355	61.25 (61.01)	4.33 (4.19)	6.24 (6.47)
[Zn(L ¹)]·2H ₂ O	Gray	195	87.6	4.43	---	271	360	59.87 (60.08)	4.47 (4.13)	6.52 (6.37)

When compared to the reference drug (Ciprofloxacin), the Schiff base shows moderate antibacterial activity against *Staphylococcus aureus* and *Escherichia coli* with respective inhibition zones of 14 mm and 11 mm at higher concentrations (Table 2). However, the results of the complexes indicated that [Co(L¹)]·3H₂O, [Ni(L¹)]·4H₂O and [Zn(L¹)]·2H₂O complexes are much more antibacterial active than [Cu(L¹)]·3H₂O. Moreover, [Co(L¹)]·3H₂O complex shows the highest antibacterial activity against all bacteria tested with a clear inhibition zones, indicating no bacterial growth within the clear zone. This could be due to the higher stability of the complex. The Schiff base, shows no activity against *Aspergillus flavus* but shows moderate activity against *Aspergillus niger*. The [Ni(L¹)]·4H₂O complex inhibits growth the most against *Aspergillus flavus*, while [Cu(L¹)]·3H₂O complex has no activity against *Aspergillus flavus* when compared to the reference drug (ketoconazole) Table 2. Similar results were reported by Aiyelabola *et al.*, [39].

The antibacterial activity of Schiff base compounds has been linked to the azomethine group in the Schiff base compound [46]. The overlapping of ligand orbitals with metal orbitals in the complex improved the antibacterial activity of the complex, allowing for partial sharing of the positive charge of metals with the donor group on the ligand. This coordination reduces the polarity of the metal, making it more lipophilic to the lipid layer of the bacterial cell membrane [47]. The increased lipophilicity allows the complexes to penetrate deeper into the lipid membrane, limiting the bacteria's ability to multiply further. The effectiveness of different compounds against different organisms varies depending on the microorganism's cells or changes in ribosome of microbial cells.

Table 2. Antibacterial and antifungal activities of Schiff base and its complexes showing the inhibition zones (mm) against the isolates.

Antibacterial activity results						
Compound	<i>Escherichia coli</i>			<i>Staphylococcus aureus</i>		
	60 mg mL ⁻¹	30 mg mL ⁻¹	15 mg mL ⁻¹	60 mg mL ⁻¹	30 mg mL ⁻¹	15 mg mL ⁻¹
Ciprofloxacin(standard)		43			40	
DMSO (control)	-	-	-	-	-	-
H ₂ (L ¹)	14	12	10	11	09	-
[Co(L ¹)]·3H ₂ O	18	15	13	17	14	12
[Ni(L ¹)]·4H ₂ O	16	14	10	17	13	11
[Cu(L ¹)]·3H ₂ O	-	-	-	09	-	-
[Zn(L ¹)]·2H ₂ O	18	16	13	15	13	12
Antifungal activity results						
	<i>Aspergillus flavus</i>			<i>Aspergillus niger</i>		
		44			36	
Ketoconazole (standard)						
DMSO (Control)	-	-	-	-	-	-
H ₂ (L ¹)	-	-	-	17	15	12
[Co(L ¹)]·3H ₂ O	24	21	17	28	24	21
[Ni(L ¹)]·4H ₂ O	29	27	20	15	12	10
[Cu(L ¹)]·3H ₂ O	-	-	-	11	09	08
[Zn(L ¹)]·2H ₂ O	22	20	16	23	19	15

CONCLUSION

Solvent-assisted mechanochemical synthesis was used to successfully synthesize the compounds, and the assisting solvent played a significant role in the synthesis. Although all the assisting solvents (methanol, water, and DMF) used, resulted in the transformation of the precursors to the target compounds, the degree of crystallinity and phase purity of the synthesized Schiff base and complexes are different. Among all the solvents, DMF solvent results in the formation of target compounds with higher degree of crystallinity as compared to other solvents, as evident from the PXRD spectra. Further, the paper highlighted that multi-step synthetic techniques are possible using mechanochemical synthesis, reducing the demand for solvents as reaction media. Thermal and spectroscopic properties of the synthesized complexes were similar. It has been shown that, under the same conditions, the [Cu(L¹)]·3H₂O complex has a higher thermal stability. *In vitro* antimicrobial study revealed that some complexes have potent antibacterial and antifungal activities against the organisms tested at various concentrations. As a result, the complexes could potentially be used as antibiotics.

ACKNOWLEDGEMENTS

The authors thank Department of Chemistry, University of Malaya for characterization of samples and Usmanu Danfodiyo University, Sokoto for funding the research work.

REFERENCES

- Sheldon, R.A. green solvents for sustainable organic synthesis: State of the art. *Green Chem.* **2005**, *7*, 267–278.
- Luo, M.; Li, H.M. One-pot synthesis and biological and catalytic applications of organometallic complexes involving oxazolines and (R)/(S)-a-phenylethylamine. *J. Iran. Chem. Soc.* **2020**, *17*, 963–971.

3. Sani, S.; Kurawa, M.A.; Siraj, I.T. Solid state synthesis, spectroscopic and X-ray studies of Cu(II) Schiff base complex derived from 2-hydroxy-3-methoxybenzaldehyde and 1, 3-phenylenediamine. *ChemSearch J.* **2018**, *9*, 76–82.
4. Bowmaker, G.A.; Chaichit, N.; Pakawatchai, C.; Skelton, B.W.; White, A.H. Solvent-assisted mechanochemical synthesis of metal complexes. *Dalton Trans.* **2008**, 2926–2928.
5. Chieng, N.; Rades, T.; Aaltonen, J. An overview of recent studies on the analysis of pharmaceutical polymorphs. *J. Pharm. Biomed. Anal.* **2011**, *55*, 618–644.
6. Friščić, T. Supramolecular concepts and new techniques in mechanochemistry: Cocrystals, cages, rotaxanes, open metal–organic frameworks. *Chem. Soc. Rev.* **2012**, *41*, 3493–3510.
7. Friščić, T. New opportunities for materials synthesis using mechanochemistry. *J. Mater. Chem.* **2010**, *20*, 7599–7605.
8. Shan, N.; Toda, F.; Jones, W. Mechanochemistry and co-crystal formation: Effect of solvent on reaction kinetics. *Chem. Commun.* **2002**, 2372–2373.
9. James, S.L.; Adams, C.J.; Bolm, C.; Braga, D.; Collier, P.; Friščić, T.; Grepioni, F.; Harris, K.D.; Hyett, G.; Jones, W. Mechanochemistry: Opportunities for new and cleaner synthesis. *Chem. Soc. Rev.* **2012**, *41*, 413–447.
10. Alekshun, M.N.; Levy, S.B. Molecular mechanisms of antibacterial multidrug resistance. *Cell* **2007**, *128*, 1037–1050.
11. Baquero, F. Gram-positive resistance: Challenge for the development of new antibiotics. *J. Antimicrob. Chemother.* **1997**, *39*, 1–6.
12. Sundriyal, S.; Sharma, R.K.; Jain, R. Current advances in antifungal targets and drug development. *Curr. Med. Chem.* **2006**, *13*, 1321–1335.
13. Nucci, M.; Marr, K.A. Emerging fungal diseases. *Clin. Infect. Dis.* **2005**, *41*, 521–526.
14. Rice, L.B. Unmet medical needs in antibacterial therapy. *Biochem. Pharmacol.* **2006**, *71*, 991–995.
15. Li, R.; Liu, S.; Du, B.; Wu, W.; Li, B.; Wang, L. Synthesis, structures and magnetic properties of cobalt(II) complexes derived from 5-(4-(1-(carboxymethyl)-1H-pyrazol-3-yl) phenyl) isophthalic acid ligand. *Transit. Met. Chem.* **2019**, *45*, 203–210.
16. Chang, J.; Zhang, S.-Z.; Wu, Y.; Zhang, H.-J.; Sun, Y.-X. Three supramolecular trinuclear nickel(II) complexes based on salamo-type chelating ligand: syntheses, crystal structures, solvent effect, Hirshfeld surface analysis and DFT calculation. *Transit. Met. Chem.* **2020**, *45*, 279–293.
17. Sun, R.W.-Y.; Zhang, M.; Li, D.; Li, M.; Wong, A.S.-T. Enhanced anti-cancer activities of a gold(III) pyrrolidinedithiocarbamate complex incorporated in a biodegradable metal-organic framework. *J. Inorg. Biochem.* **2016**, *163*, 1–7.
18. Ganguly, R.; Sreenivasulu, B.; Vittal, J.J. Amino acid-containing reduced Schiff bases as the building blocks for metallasupramolecular structures. *Coord. Chem. Rev.* **2008**, *252*, 1027–1050.
19. Massai, L.; Pratesi, A.; Bogojeski, J.; Banchini, M.; Pillozzi, S.; Messori, L.; Bugarčić, Ž.D. Antiproliferative properties and biomolecular interactions of three Pd(II) and Pt(II) complexes. *J. Inorg. Biochem.* **2016**, *165*, 1–6.
20. Alibrahim, K.A.; Alsuhaibani, A.M.; Refat, M.S. Synthesis and spectroscopic characterizations of manganese(II), iron(III), copper(II) and zinc(II) hydrazine complexes as catalytic activity agents. *Bull. Chem. Soc. Ethiop.* **2022**, *36*, 33–44.
21. Souza, A.O. de; Galetti, F.; Silva, C.L.; Bicalho, B.; Parma, M.M.; Fonseca, S.F.; Marsaioli, A.J.; Trindade, A.C.; Gil, R.P.F.; Bezerra, F.S. Antimycobacterial and cytotoxicity activity of synthetic and natural compounds. *Quím. Nova* **2007**, *30*, 1563–1566.
22. Wang, C.; Wu, Y.; Qu, Y.; Zhao, K.; Xu, J.; Xia, X.; Wu, H. Synthesis, structure and antioxidant properties of manganese(II), zinc(II) and cobalt(II) complexes with bis (benzimidazol-2-ylmethyl) allylamine. *Transit. Met. Chem.* **2020**, *45*, 523–529.

23. Bottari, B.; Maccari, R.; Monforte, F.; Ottanà, R.; Rotondo, E.; Vigorita, M.G. Antimycobacterial in vitro activity of cobalt(II) isonicotinoylhydrazone complexes. Part 10. *Bioorg. Med. Chem. Lett.* **2001**, *11*, 301–303.
24. Cockerill III, F.R.; Uhl, J.R.; Temesgen, Z.; Zhang, Y.; Stockman, L.; Roberts, G.D.; Williams, D.L.; Kline, B.C. Rapid identification of a point mutation of the mycobacterium tuberculosis catalase-peroxidase (KatG) gene associated with isoniazid resistance. *J. Infect. Dis.* **1995**, *171*, 240–245.
25. Mali, R.K.; Somani, R.R.; Toraskar, M.P.; Mali, K.K.; Naik, P.P.; Shirodkar, P.Y. Synthesis of some antifungal and anti-tubercular 1,2,4-triazole analogues. *Int. J. Chem. Technol. Res.* **2009**, *1*, 168–173.
26. Sidhaye, R.V.; Dhanawade, A.E.; Manasa, K.; Aishwarya, G. Synthesis, antimicrobial and antimycobacterial activity of nicotinic acid hydrazide derivatives. *J. Curr. Pharma Res.* **2011**, *1*, 135–139.
27. Aftab, M.; Mazhar, N.; Shah, M.T.; Batool, M.A.M.; Mahmud, T.; Basra, M.A.R.; Bratu, G.; Mitu, L. Synthesis, characterization and biological evaluation of three new Schiff bases derived from amino acids and their Ag(I) complexes. *Bull. Chem. Soc. Ethiop.* **2022**, *36*, 45–56.
28. Sirajuddin, M.; Ahmad, C.; Khan, H.; Ullahkhan, I.; Tariq, M.; Ullah, N. Synthesis, spectroscopic characterization, biological screening and POM analysis of potentially bioactive copper(II) carboxylate complexes. *Bull. Chem. Soc. Ethiop.* **2022**, *36*, 57–71.
29. Yusha'u, M.; Sadiu, F.U. Inhibition activity of detarium microcarpum extracts on some clinical bacterial isolates. *Biol. Environ. Sci. J. Trop.* **2011**, *8*, 113–117.
30. Cinčić, D.; Kaitner, B. Schiff base derived from 2-hydroxy-1-naphthaldehyde and liquid-assisted mechanochemical synthesis of its isostructural Cu(II) and Co(II) complexes. *CrystEngComm* **2011**, *13*, 4351–4357.
31. Kaitner, B.; Zbačnik, M. Solvent-free mechanochemical synthesis of two thermochromic Schiff bases. *Acta Chim. Slov.* **2012**, *59*, 670–679.
32. Nejo, A.A.; Kolawole, G.A.; Nejo, A.O. Synthesis, characterization, antibacterial, and thermal studies of unsymmetrical Schiff-base complexes of cobalt(II). *J. Coord. Chem.* **2010**, *63*, 4398–4410.
33. Vadivel, T.; Dhamodaran, M. Synthesis, characterization and antibacterial studies of ruthenium(III) complexes derived from chitosan Schiff base. *Int. J. Biol. Macromol.* **2016**, *90*, 44–52.
34. Joseyphus, R.S.; Dhanaraj, C.J.; Nair, M.S. Synthesis and characterization of some Schiff base transition metal complexes derived from vanillin and L (+) alanine. *Transit. Met. Chem.* **2006**, *31*, 699–702.
35. Reddy, V.; Patil, N.; Angadi, S.D. Synthesis, characterization and antimicrobial activity of Cu(II), Co(II) and Ni(II) complexes with O, N, and S donor ligands. *J. Chem.* **2008**, *5*, 577–583.
36. Nakamoto, K. *Infrared and Raman Spectra of Inorganic and Coordination Compounds. Handbook of Vibrational Spectroscopy*, John Wiley and Sons: New York; **2006**.
37. Joseyphus, R.S.; Nair, M.S. Synthesis, characterization and biological studies of some Co(II), Ni(II) and Cu(II) complexes derived from indole-3-carboxaldehyde and glycylglycine as Schiff base ligand. *Arab. J. Chem.* **2010**, *3*, 195–204.
38. Ghorbani-Choghamarani, A.; Darvishnejad, Z.; Tahmasbi, B. Schiff base complexes of Ni, Co, Cr, Cd and Zn supported on magnetic nanoparticles: As efficient and recyclable catalysts for the oxidation of sulfides and oxidative coupling of thiols. *Inorganica Chim. Acta* **2015**, *435*, 223–231.
39. Aiyelabola, T.O.; Ojo, I.A.; Adebajo, A.C.; Ogunlusi, G.O.; Oyetunji, O.; Akinkunmi, E.O.; Adeoye, A.O. Synthesis, characterization and antimicrobial activities of some metal(II) amino acids' complexes. *Adv. Biol. Chem.* **2012**, *2*, 268–273.

40. Khalil, M.M.; Ismail, E.H.; Mohamed, G.G.; Zayed, E.M.; Badr, A. Synthesis and characterization of a novel Schiff base metal complexes and their application in determination of iron in different types of natural water. *Open J. Inorg. Chem.* **2012**, *2*, 13–21.
41. Shaker, S.A.; Aziz, Y.F.A.; Salleh, A.A. Synthesis and characterization of mixed ligand complexes of 8-hydroxyquinoline and o-hydroxybenzylidene-1-phenyl-2, 3-dimethyl-4-amino-3-pyrazolin-5-on with Fe(II), Co(II), Ni(II) and Cu(II) Ions. *Eur. J. Sci. Res.* **2009**, *33*, 702–709.
42. Kalia, S.B.; Lumba, K.; Kaushal, G.; Sharma, M. Magnetic and spectral studies on cobalt(II) chelates of a dithiocarbazate derived from isoniazid. **2007**, *46A*, 1233–1239.
43. Carabineiro, S.A.; Silva, L.C.; Gomes, P.T.; Pereira, L.C.; Veiros, L.F.; Pascu, S.I.; Duarte, M.T.; Namorado, S.; Henriques, R.T. Synthesis and characterization of tetrahedral and square planar bis (iminopyrrolyl) complexes of cobalt(II). *Inorg. Chem.* **2007**, *46*, 6880–6890.
44. Tas, E.; Aslanoglu, M.; Kilic, A.; Kara, Z. Synthesis, spectroscopic and electrochemical studies of copper(II) and cobalt(II) complexes of three unsymmetrical vic-dioximes ligands. *J. Coord. Chem.* **2006**, *59*, 861–872.
45. Bhowon, M.G.; Wah, H.L.K.; Narain, R. Schiff base complexes of ruthenium(II) and their use as catalytic oxidants. *Polyhedron* **1998**, *18*, 341–345.
46. Guo, Z.; Xing, R.; Liu, S.; Zhong, Z.; Ji, X.; Wang, L.; Li, P. Antifungal properties of Schiff bases of chitosan, N-substituted chitosan and quaternized chitosan. *Carbohydr. Res.* **2007**, *342*, 1329–1332.
47. Nishat, N.; Hasnain, S.; Ahmad, T.; Parveen, A. Synthesis, characterization, and biological evaluation of new polyester containing Schiff base metal complexes. *J. Therm. Anal. Calorim.* **2011**, *105*, 969–979.